BEHAVIOUR OF BERYLLIUM IN A TOKAMAK FUSION REACTOR

Yip Hoi-tung*

IPP 6/228 June 1983

MAX-PLANCK-INSTITUT FÜR PLASMAPHYSIK

8046 GARCHING BEI MÜNCHEN

MAX-PLANCK-INSTITUT FÜR PLASMAPHYSIK

GARCHING BEI MÜNCHEN

BEHAVIOUR OF BERYLLIUM IN A TOKAMAK FUSION REACTOR

Yip Hoi-tung*

IPP 6/228 June 1983

*Department of Nuclear Engineering
Kyoto University, Kyoto 606, Japan

Die nachstehende Arbeit wurde im Rahmen des Vertrages zwischen dem Max-Planck-Institut für Plasmaphysik und der Europäischen Atomgemeinschaft über die Zusammenarbeit auf dem Gebiete der Plasmaphysik durchgeführt.

Contents

Yip Hoi-tung+

BEHAVIOUR OF BERYLLIUM IN A TOKAMAK FUSION REACTOR

June 1983
(in English)

Abstract

The behaviour of beryllium in a fusion plasma was studied by using the BITC (Bologna Impurity Transport Code) code for the parameters of the JET. The radial profiles of Z-effective, ionization states and fluxes are given. The radiation losses by the beryllium impurity in a fusion reactor are estimated less than 1% of the total power input. The radiation losses by beryllium in corona equilibrium are also presented.

1. Introduction

Energetic charged particles, neutral particles and neutrons leak from the plasma will bombard the metallic wall of the vaccum chamber, hence the metallic atoms of the wall will be sputtered out of the wall and enter into the plasma column. This causes the contamination of the plasma and the erosion of the wall.

Impurity radiation from a fusion plasma represents a large fraction of the total power input. Hugill recently in his review paper[1)] summarized some typical published data which show that at the wurst case the radiation power by impurity is as large as the total power input; even in "clean" discharges, it is rarely less 15% of the total power input.

Impurities also effect the fusion power density hence the total power output, and the particle heating, since both of these are proportional to n_i^2, where n_i is the main plasma ion density. The relation $n_e = n_i + Z_{im} n_{im}$, where n_e is electron density, Z_{im} and n_{im} are the atomic number and density of an impurity, respectively, implies that high-Z impurity may efficiently reduce the ratio of n_i/n_e. Meade's investigation[2)] shows that tungsten (Z=74) with a level of 0.2% of electron density or molybdenum (Z = 42) with a level of 0.8% of electron density will prevent the plasma from ignition at any temperature. Therefore, how to reduce both of the density and the

Z-value of impurity has a strategical meaning for the fusion reactor design. For the first purpose, a promising method, i.e. the poloidal divertor was developed to control the impurity density[3], through this will bring complexity to the fusion reactor design.

As to the second purpose, there is nothing to do but choose low-Z materials to build a first solid layer facing the plasma column. In fact, in some fusion reactor design, no divertor is considered[4], instead, a carbon (Z = 6) curtain setting between the plasma and the first wall was proposed by Kulcinski et al.[5].

Beryllium also is considered as a material for coating the limiter and the first wall.[6] Hence it is probably that beryllium impurity will exist in the plasma of a fusion reactor. As a material for fusion reactor, the most attractive properties of beryllium are of its low atomic number, its low neutron capture cross-section and its high strength-to-weight ratio. Beryllium, symbol Be, is one of the uncommon metallic elements. Its atomic number is 4, in the second group of the Periodic Table. Some physical properties of metallic beryllium are listed in Table 1,[8] in comparision, that of the other elements in the same group are also listed. A comparison of beryllium with other pure metals is shown in Table II[9]. From Tables I and II[+] we can see that as a light metal, the melting point of beryllium is dramatically high , its elastic modulus even larger than that of iron.

The Thermal neutron absorption cross-section of beryllium is 0.01 barn[10]. Further details about the properties of beryllium are given in Ref. 6.

In this paper, we are going to use the BITC impurity transport code[7] to simulate the beryllium behaviour in a fusion plasma as well as its radiation losses.

+) In Tables I and II, some properties of an element have different values, this is probably due to experimental conditions.

Table I. Some physical properties of beryllium and other alkaline earth elements.

Symbol	Be	Mg	Ca	Sr	Ba	Ra
Atomic No.	4	12	20	38	56	88
Atomic weight	9.013	24.32	40.08	87.63	137.36	226.05
Density g/cm^3 at 20 °C	1.848	1.74	1.55	2.6	3.5	5.0
melting point °C	1277	650±2	838	786	714	700
specific heat cal/g/ °C at 20 °C	0.45	0.245	0.149	0.176	0.068	-
heat of fusion cal/g	260	88±2	52	25	-	-
coefficient of liner expansion 25-100 °C μ in/in/°C	11.6	27.1	22.3	-	-	-
electrical resistivity μ-ohm-cm at 20 °C	4	4.45	-	23	-	-
Modulus of elasticity at 20 °C Mlb/in^2	44	6.35	3.2-3.8	-	-	-

Table II. Some physical properties of beryllium and other metallic elements.

Property	Unit	Be	Al	Cu	Fe	Ti
Melting point	°C	1287	660	1083	1535	1678
Relative density (d)		1.85	2.70	8.96	7.87	4.51
Elastic modulus (E) GPa		295	70	130	211	120
Specific modulus (E/d)		160	26	14	27	26
Mean specific heat 0-100°C	$J\ Kg^{-1}K^{-1}$	2052	917	386	456	528
Thermal conductivity 20-100°C	$Wm^{-1}K^{-1}$	194	238	397	78	26
Coefficient of thermal expansion 0-100°C	$10^{-6}K^{-1}$	12.0	23.5	17.0	12.1	8.9
Electrical resistivity at 20°C	$\mu ohm \cdot cm^{-1}$	3.3	2.67	1.69	10.1	54

2. Simulation Model

The BITC Code is an one-dimensional impurity transport code which computes the time evolution of the radial densities of impurities present in a Tokamak plasma. The radiation losses in which including the line radiation, radiative recomiration radiation and bremstrahlung are also calculated. The transport model and the mathematical treatments of the BITC Code is described in reference 7. In using this Code to simulate the beryllium transport in a fusion reactor, the specification is given below :

(1) The radial profiles of the plasma density and the temperature are

$$n_e(r) = 0.9\, n_{eo}\left(1 - \frac{r^2}{a^2}\right) + 0.1\, n_{eo}$$

$$T_i(r) = T_e(r) = 0.99\, T_{eo}\left(1 - \frac{r^2}{a^2}\right)^2 + 0.01\, T_{eo}$$

where a is the minor radius of the torus, for JET, its value is 162 cm. Other parameters for JET are

Major radius $R = 296$ cm ,

Toroidal magnetic field $B_t = 34.5$ KG ,

Total plasma current $I_p = 4.8$ MA .

n_{eo} is fixed to be $5 \times 10^{13}\,cm^{-3}$, T_{eo} is treated as a parameter and changed in the range of fusion interest, $T_{eo} = 1, 5, 10, 20, 50$ (keV).

(2) Initial impurity profile

The constraint applied to the initial impurity profile is

$$\sum_k n_k(r) = N$$

where $n_k(r)$ is the concentration of radius, r, of the kth ionization state of the impurity species and N is some specified constant. In this calculation, N is set to be 1% of the value of n_{eo}, namely $5 \times 10^{11} cm^{-3}$.

(3) Boundary conditions

The influx of neutral impurity atoms, Γ^{in} is specified as

$$\Gamma^{in} = \Gamma_0 + R\left|\sum_K \Gamma_K(r=a)\right|$$

where Γ_0 is an imposed influx, $\Gamma_K(r = a) = n_k v_{eff}$, ($v_{eff} = 5000\ cms^{-1}$) is the outflux of the kth stage of ionization of the impurity at the boundary (r = a) and R is here the recycling coefficient. In our calculation their values are

$$\Gamma_0 = 0, \qquad R = 1.$$

The values of diffusion coefficient and the inward velocity are supposed to be 5000 cms^{-1} and 0, respectively.

3. Rate coefficients for atomic processes

In evaluating the ionization state of impurities and the power radiated, the rate coefficients for atomic processes are need. For the direct electron impact ionization, the rate coefficient S_Z of an ion of charge Z is given by the formula[11)]

$$S_Z = 6.7\times10^{-7}\sum_{i=1}^{N}\frac{a_i q_i}{T_e^{3/2}}\left\{\frac{E_1(u_i)}{u_i} - \frac{b_i \exp(c_i)}{u_i + c_i}E_1(u_i + c_i)\right\} \quad (\mathrm{cm^3 s^{-1}}) \qquad (1)$$

where $u_i = P_i/T_e$ and P_i is the ionization energy of electrons in the ith subshell, and q_i the number of equivalent electrons in that shell; T_e is the electron temperature ; N is the number of peripheral subshells contributing to the ionization. The subshell ionization energies P_i for the elements from hydrogen to zinc and the coefficients a_i, b_i, c_i are given by Lotz[11), 12)]. And E_1 is the exponential integral expressed as $E_1(x) = \int_x^{\infty}\frac{e^{-t}}{t}dt$.

Data for beryllium are listed in Table III.

The rate coefficient of radiative recombination is given by Griem[13)],

$$R_r^Z = 5\times10^{14} Z^4\left(\frac{E_H}{T_e}\right)^{3/2}\left\{\frac{1}{n_z^3}\left(1-\frac{q_z}{2n_z^2}\right)\exp\left(\frac{Z^2E_H}{n_z^2T_e}\right)E_1\left(\frac{E_{nn'}}{T_e}\right) + \sum_{n_z+1}^{n'}\frac{1}{n}\exp\left(\frac{Z^2E_H}{n^2T_e}\right)E_1\left(\frac{E_{nn'}}{T_e}\right)\right\}, \quad (\mathrm{cm^3 s^{-1}}) \qquad (2)$$

where Z is the charge of the recombination ion; E_H is the ionization energy of hydrogen ; n_z and q_z are the principal quantum number and the number of electrons, in the outer main shell, respectively ;n' and $E_{nn'}$ are the effective principal quantum number and the excitation energy, respectively, and can be computed by the formulas,

$$n' \simeq 1.26 \times 10^2 \, Z^{14/17} \left(\frac{T_e}{Z^2 E_H} \right)^{1/17} \exp\left(\frac{4}{17} \frac{Z^2 E_H}{T_e} \frac{1}{n'^3} \right) \qquad (3)$$

$$\frac{E_{nn'}}{T_e} = \left[\frac{1}{n^2} - \frac{1}{(n'+1)^2} \right] \frac{Z^2 E_H}{T_e} \, . \qquad (4)$$

Table III Data for Collisional ionization

	IP(EV)	NNG	A	B	C
BE I					
	9.3	2	4.00	0.70	0.50
	114.0	2	4.20	0.60	0.60
	0.0	0	0.00	0.00	0.00
BE II					
	18.2	1	4.40	0.00	0.00
	124.0	2	4.00	0.40	0.60
	0.0	0	0.00	0.00	0.00
BE III					
	153.9	2	4.5	0.3	0.60
	0.0	0	0.0	0.0	0.00
	0.0	0	0.0	0.0	0.00
BE IV					
	217.7	1	4.5	0.0	0.00
	0.0	0	0.0	0.0	0.00
	0.0	0	0.0	0.0	0.00
BE V					
	0.0	0	0.0	0.0	0.00
	0.0	0	0.0	0.0	0.00
	0.0	0	0.0	0.0	0.00

IP : ionization energy ; NNG : number of equivalent electrons in the subshell

A, B, C, : coefficients given by Lotz

The rate coefficient of dielectronic recombination is calculated by the formula which proposed by Burgress[14),]

$$R_d^Z = 2.4 \times 10^{-9} T_e^{-3/2} B(Z) \sum_{i,j} f_{ij} A(x) \exp(\bar{E}/T_e) \ (cm^3 s^{-1}) \quad (5)$$

where

$$B(Z) = Z^{1/2} (Z+1)^{5/2} (Z^2 + 13.4)^{-1/2}$$

$$A(x) = x^{1/2} / (1.0 + 0.105 X + 0.015 x^2) \ ; \ x = E_{ij} / E_H (1+Z)$$

$$\bar{E} = E_{ij} / \alpha$$

$$\alpha = 1. + 0.015 Z^3 / (Z+1)^2.$$

The sum is over the resonance transitions $i \to j$ with E_{ij} and f_{ij} are the excitation energy and the oscillator strength, respectively. Data for beryllium are taken from references 15 and 16 and listed in Table IV.

Table IV Data for dielectronic Recombination.

	R.TRANSITION	E(EV)	F	NDEL
BE I				
	2S - 2P	4.5	1.9580	0
	2P - 3S	5.2	0.1640	1
BE II				
	2S - 2P	4.0	0.5050	0
	2S - 3P	12.0	0.0800	1
	2P - 3D	12.1	0.6520	1
BE III	1S - 2P	123.6	0.5520	1
	1S - 3P	140.4	0.1270	2
BE IV				
BE V				

(E is meam excitation energy of a group of transitons;

F is the sum of the oscillator strengths of the transitions;

NDEL is the change of the principal quantum number in the transition.)

4. Numerical Results

Figures 1 through 5 show the numerical results which the impurity is considered reaching a quasi-steady state. In Figs. 1(a) to (d), we show the results for T_{eo} = 1 keV. Figure 1(a) shows the radial profiles of Z-effective. Its value varied from about 1.12 to 1.37, and has a maximum at r = 0.9a. The main value of Z-effective is approximately equal to 1.21. Figure 1(b) shows the radial profiles of the ionization states of beryllium. The Be V (Be^{+4}) ion has the largest fraction of the four ionization states of beryllium. And in region of $r<0.8a$ all ions have an almost flat radial profile. In this region impurity fluxes driven by the gradient of the impurity density are actually very small, as they are shown in Fig. 1(c).

Figure 1(d) shows the radial profiles of the radiation power densities of line radiation, radiative recombination and bremsstrahlung. Amount these radiation losses, the line ratiation is the most important one, and it has a much greater value at the periphery of the plasma column.

Changing the electron temperature, the results correspondent to Fig. 1 obtained for T_{eo} equal to 5 keV, 10 keV, 20 keV 50 keV are shown in Figs. 2,3,4 and 5, respectively. When the electron temperature increased, the radiation loss by bremsstrahlung become more important.

5. Radiation losses in corona equilibrium

In practical tokamak discharges the impurity re-cycling from the wall and the impurity transport would prevent the local corona equilibrium from being reached. However, as a radiation state, the radiation losses from a beryllium plasma at corona equilibrium are also calculated. The fractional abundances are given by

$$f_z = n_z / \sum_z n_z = n_z / n_{im} \tag{6}$$

And the balance equation can be simply written as

$$n_e n_z S_z = n_e n_{z+1} \alpha_{z+1} \tag{7}$$

Both of the fractional abundances and the coronal equilibrium depend on the electron temperature only. In Fig. 6 the fractional abundances are shown as a function of the electron temperature. When the electron temperature is greater than 70 eV , the beryllium is fully ionized.

In Fig. 7 radiation losses from beryllium plasma are expressed as the ratios $P/n_e n_{im}$ and plotted as a funtion of the electron temperature. At $T_e < 50$ eV, the line radiation is the main radiation loss, while at $T_e > 500$ eV, the bremsstrahlung becomes the dominant contribution to the radiation losses.

6. Discussion and summary

In comparison the total power radiated by beryllium with the total power input, we must compute the two powers. If we ignore the absorption by the plasma itself, the total power radiated from the whole plasma column can be expressed

$$P_{Loos} = \int P_t(r)dV = 4\pi^2 R \int_0^a P_t(r) r\,dr \qquad (8)$$

where R and a are the major radius and the minor radius of the torus, P_t is the averaged radiation power in the quasi-steady state.

The total power input including ohmic heating, neutral beam injection and RF heating can be written as

$$P_{in} = P_{OH} + P_{NBI} + P_{RF} \qquad (9)$$

The ohmic heating power can be simply calculated by the formula $P_{OH} = I_p^2 R_p$ (10)

where I_p is the total current. The resistance of the plasma column is given by

$$R_p = l\eta_p/S = 2\cdot R\eta_p/a^2 \qquad (11)$$

where l and S are the length and the cross section of the torus, η_p is the resistivity of the plasma which is given by Spitze[15].

$$\eta_p = 1.6 \times 10^{-9} Z_{eff} \ln\Lambda / T_e^{3/2} \quad \text{(ohm m)} \qquad (12)$$

where T_e is the electron temperature in KeV. From eqs. (10), (11) and (12), we get

$$P_{OH} = 3.2 \times 10^{-9} R I_p^2 Z_{eff} \ln\Lambda / T_e^{3/2} a^2 \quad \text{(Watt)} \qquad (13)$$

By assuming some special values of Z_{eff} and for the electron temperature interested, and with the parameters of JET, the power radiated by beryllium and the total power input and the ratio of P_{Loss}/P_{in} can be computed. They are listed in Table V.

Table V Total power radiated by beryllium, power input and their ratio.

T_{eo} (KeV)	1	5	10	20	50
Z_{eff}	1.21	1.20	1.11	1.11	1.11
$\ln\Lambda$	21.5	23.9	25.0	26.0	27.4
P_{OH} (MW)	2.2	0.22	0.075	0.027	7.4×10^{-3}
P_{NBI} (MW)	10	10	10	10	10
P_{RF} (MW)	15	15	15	15	15
P_{in} (MW)	27.2	25.22	25.075	25.027	25.0074
P_{Loss} (MW)	78.1×10^{-2}	4.17×10^{-2}	3.65×10^{-2}	3.81×10^{-2}	5.98×10^{-2}
P_{Loss}/P_{in} (%)	0.29	0.17	0.15	0.15	0.24

When the electron temperature increased, the Ohmic heating efficiency become wurse. At the electron temperature larger than 10 keV power radiated by beryllium is comparable with Ohmic heating power or even greater. Fortunately, with the help of neutral beam injection and RF heating, the power lost due to the radiation of the beryllium is less than 1% of the total power input.

Acknowledgement

The author would like to thank the Max-Planck-Institut für Plasmaphysik (IPP) and Prof. Dr. Pfirsch for providing a good research enviroment during the period of his staying at the IPP as a guest scientist. It is a pleasure for him to thank Drs. D. Düchs and O. DeBarbieri for their constant encouragement. He is grateful to Drs. E. Bittoni and P. O. Ottaviani for their permission of using the BITC code and help to run it. The author also wishes to acknowledge Mrs. Richter for her excellent plotting subroutines.

The numerical calculation was done by using the system Cray-1 of the Institute.

References

1) Hugill, J., Nuclear Fusion 23, No. 3 (1983) 331.

2) Meade, D., Nucl. Fus. 14 (1974) 289.

3) Shimomura, Y., Keilhacker, M., Lackner, K., Murmann, H., Siller, G., Report IPP III/80 (Dec.,1982)

4) Badger, B. et al., NUWMAK, UWFDM-330, (March 1979).

5) Kulcinski, G.L., Conn, R.W., Nucl. Fus. 15 (1974) 327.

6) Abdon, M. et al., USA FED-INTOR/82-7, Critical Issues Vol. I. (1982) Ch. VII.

7) Bittoni, E., Ottaviani, P.L., "BITC-A Fortran program for Impurity Transport in Tokamaks", in Press, also Bottoni, E., Ottaviani, P.L., and Taroni, A.,"One Dimensional code for Impurity transport and (non-coronal) Impurity Relations, TIB/FICS/MATAPPL (82) 7.

8) Simons, E.N., Guide to Uncommon Metals, Hart Publishing Co. Inc., New York (1967) 13-19.

9) Smithells, C.J. Metals References Book, 5th ed, Butterworthus, London (1976)

10) Haro Von Butter, Nuclear Physics An Introduction, A.P. New York, London (1968) Chart of Nuclides.

11) Lotz, W., Z. Phys.,216 (1968) 241-247.

12) Lotz, W., J. Astro. Phys. Suppl. series, Vol XIV, No. 128(1967) 207-237.

13) Griem, H.R., Plasma Spectroscopy, McGraw-Hill, New York (1964) 160.

14) Burgess, A., Astrophys. J. 141 (1964) 1588.

15) Wiese, W.L., Smith, M. W. and Glennon, B.M., Atomic transition probilities, Vol. I, NSRDS-NBS 4 (1966).

16) Kelley, R. L. and Palumbo, L.J., NRL-R 7599 (1973).

17) Spitze, Physics of Fully Ionized Gases, Interscience Publishers, New York, London (1962) 139.

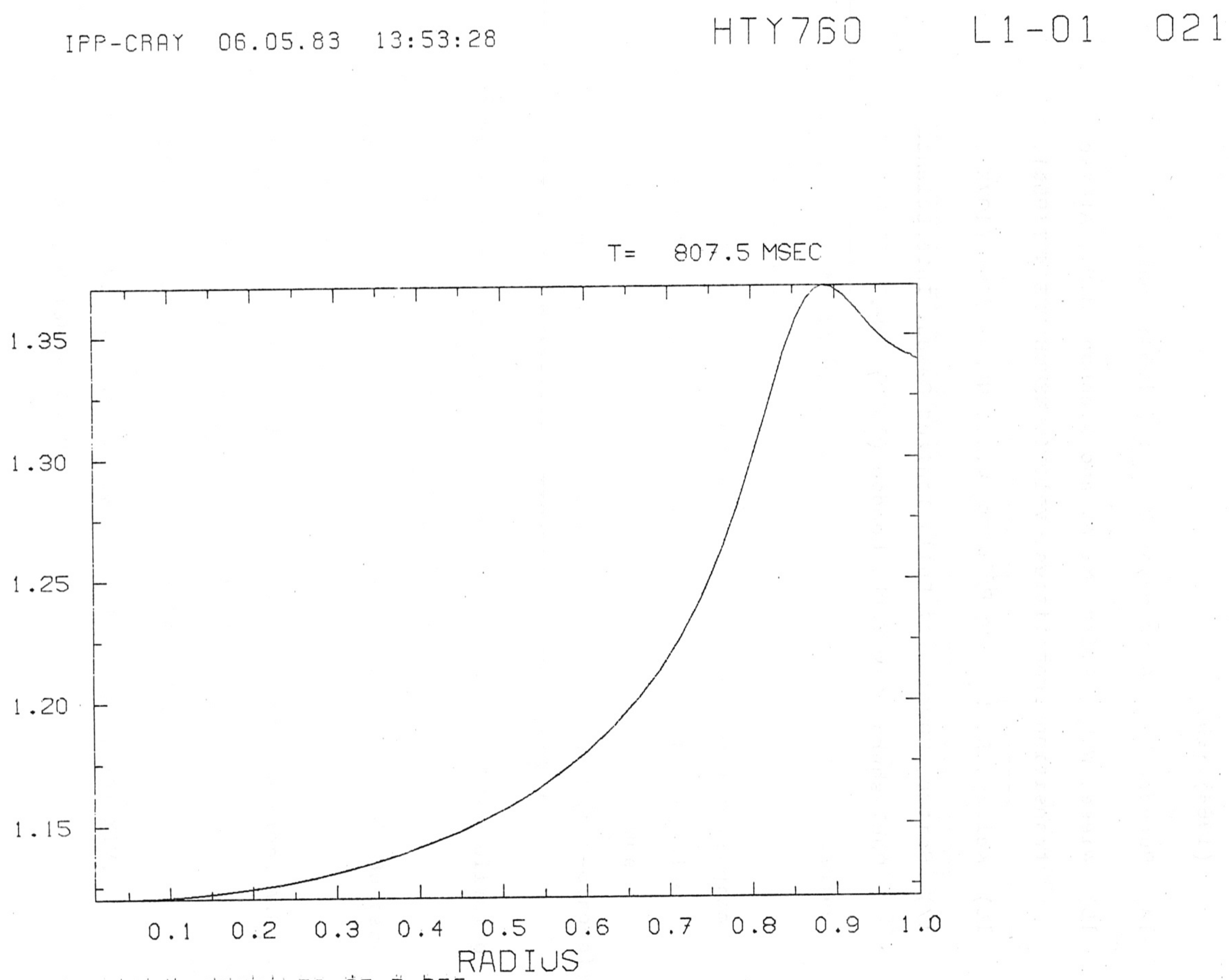

Fig.1(a) RADIAL PROFILES OF Z-EFF

IPP-CRAY 06.05.83 13:53:28 HTY760 L1-01 022

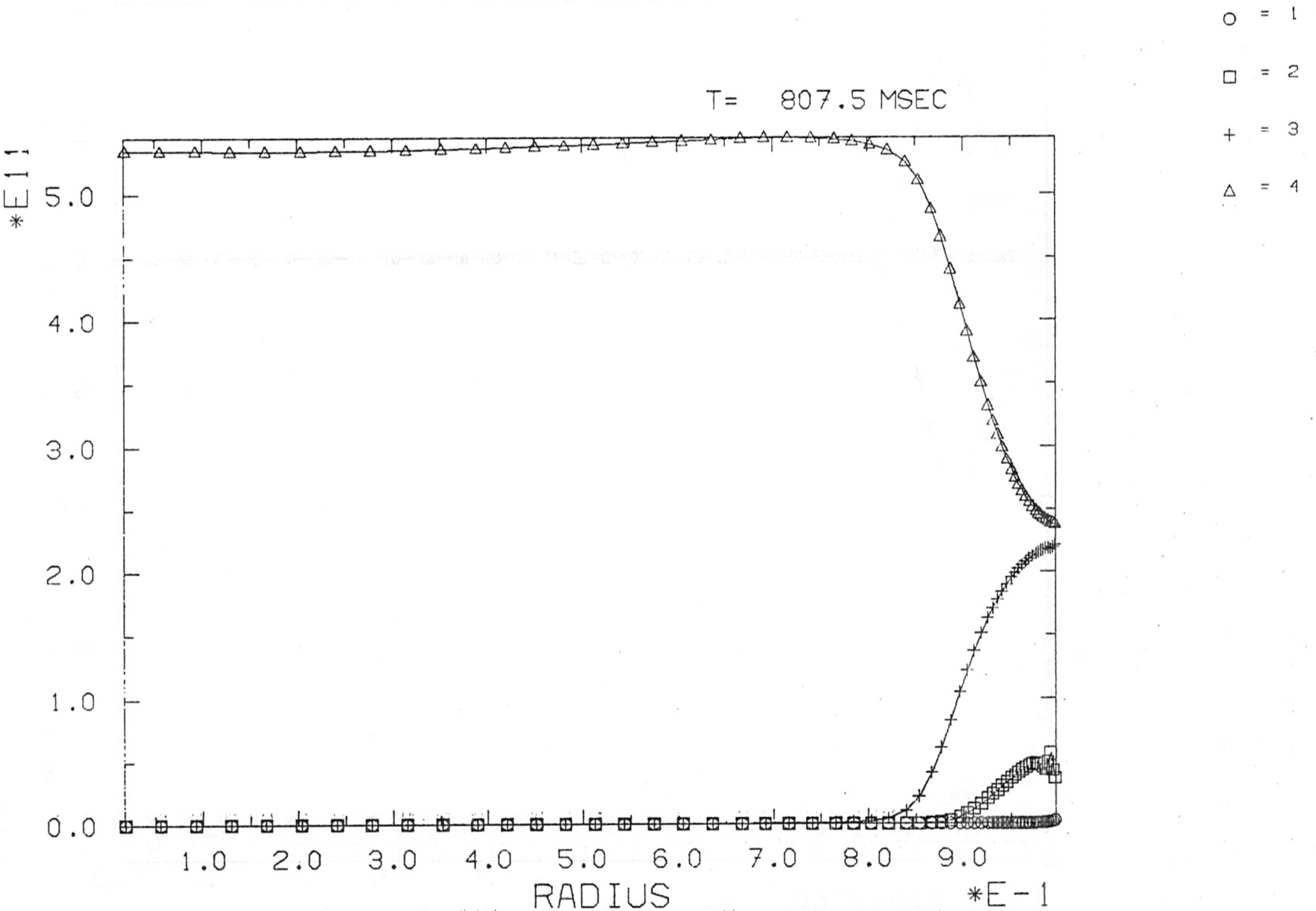

Fig.1(b) RADIAL PROFILES OF THE IMPURITY IONIZATION STATES

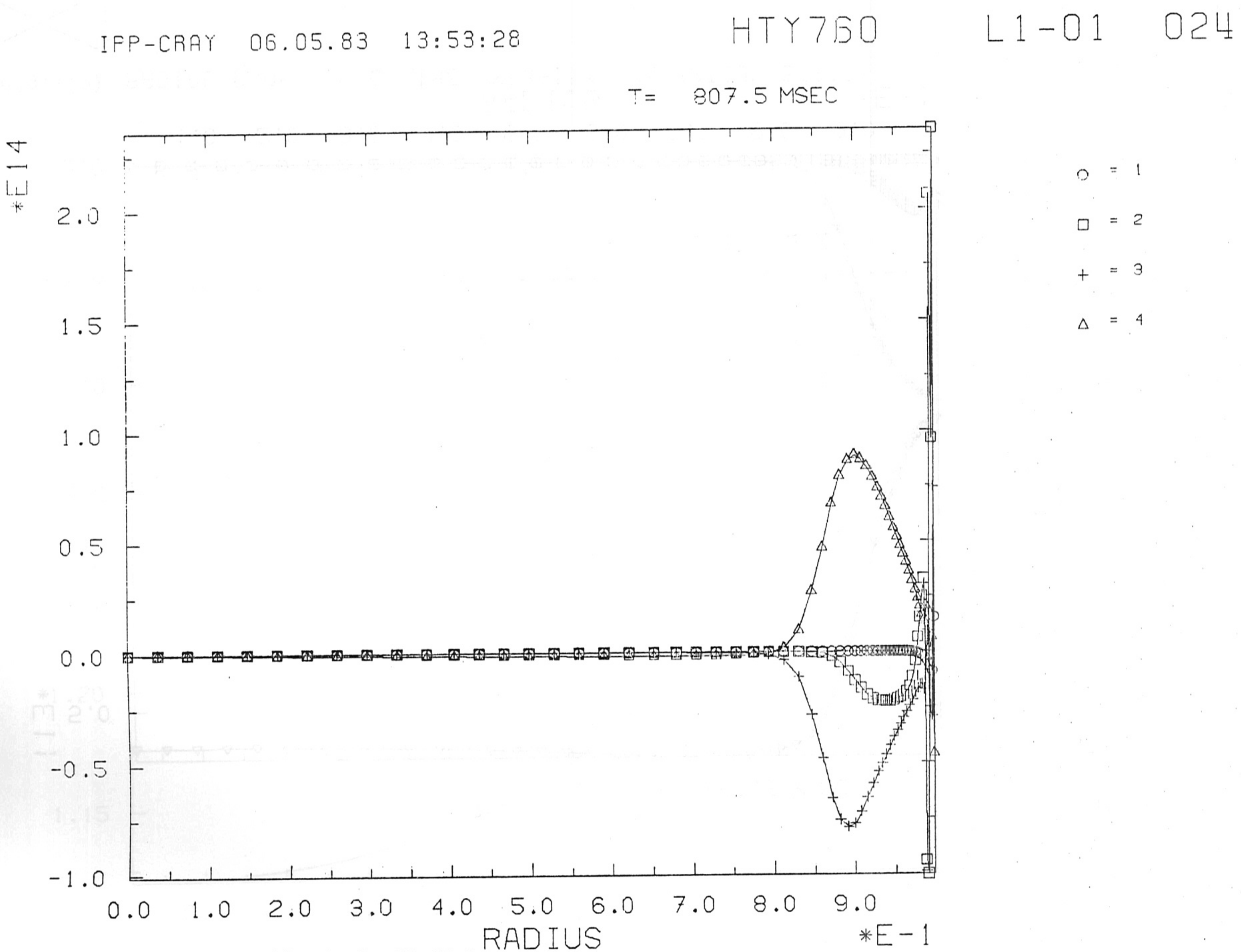

Fig.1(c) TOTAL PARTICLE FLUX DENSITY

IPP-CRAY 06.05.83 13:53:28 HTY760 L1-01 026

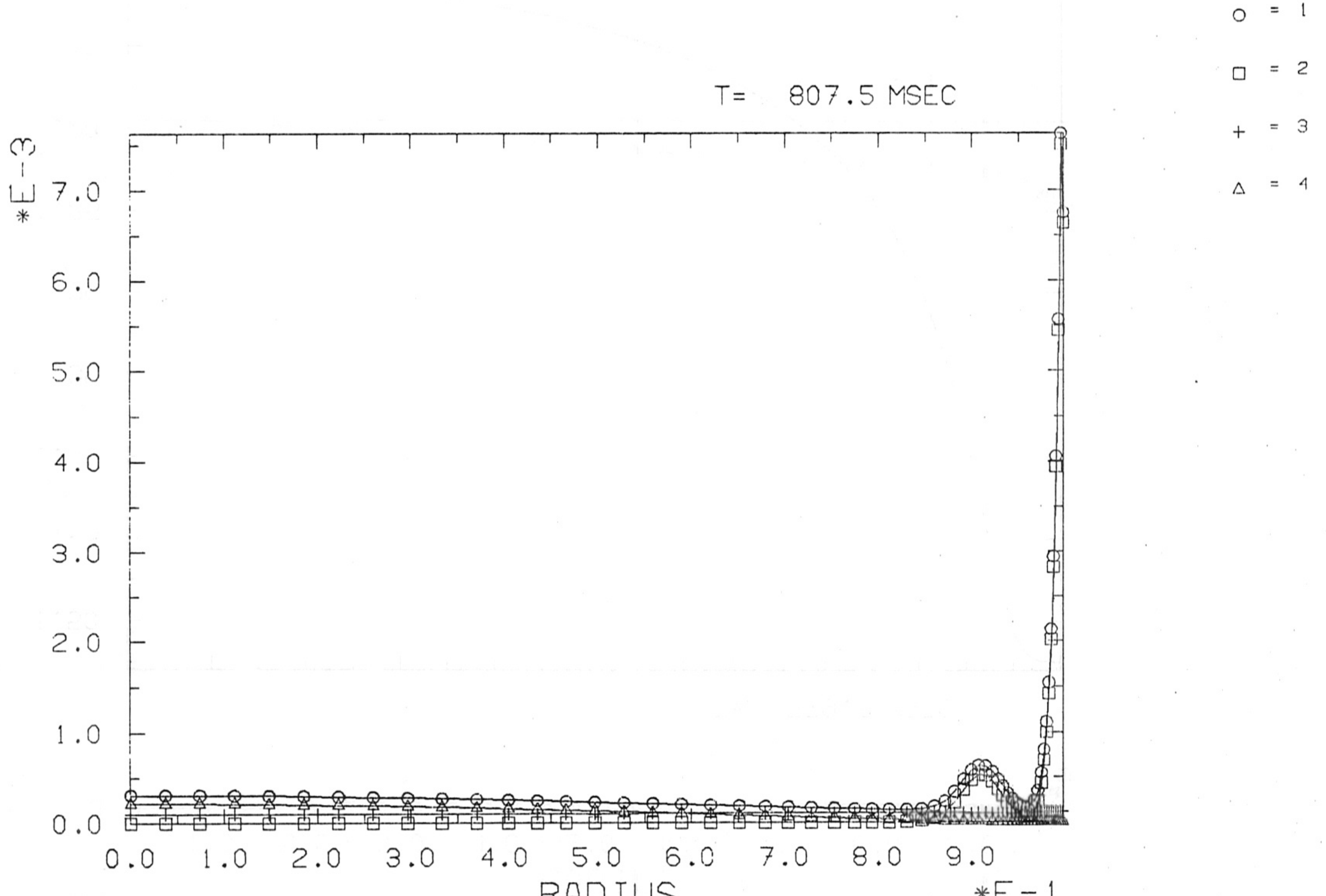

Fig.1(d) RADIATIVE ENERGY LØSS (PER UNIT VOLUME)-TOTAL.LINE.RECOM.BREMS

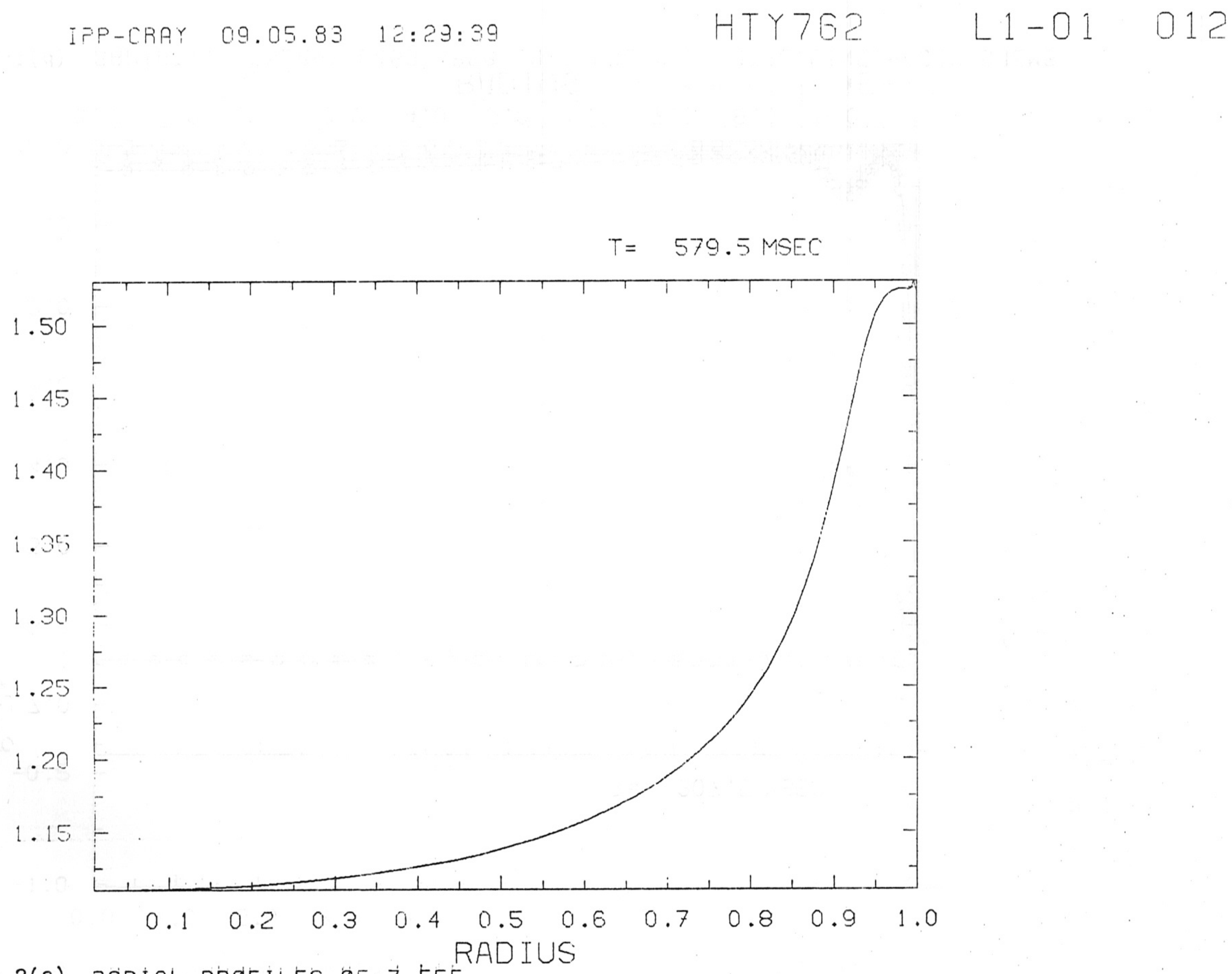

Fig.2(a) RADIAL PROFILES OF Z-EFF

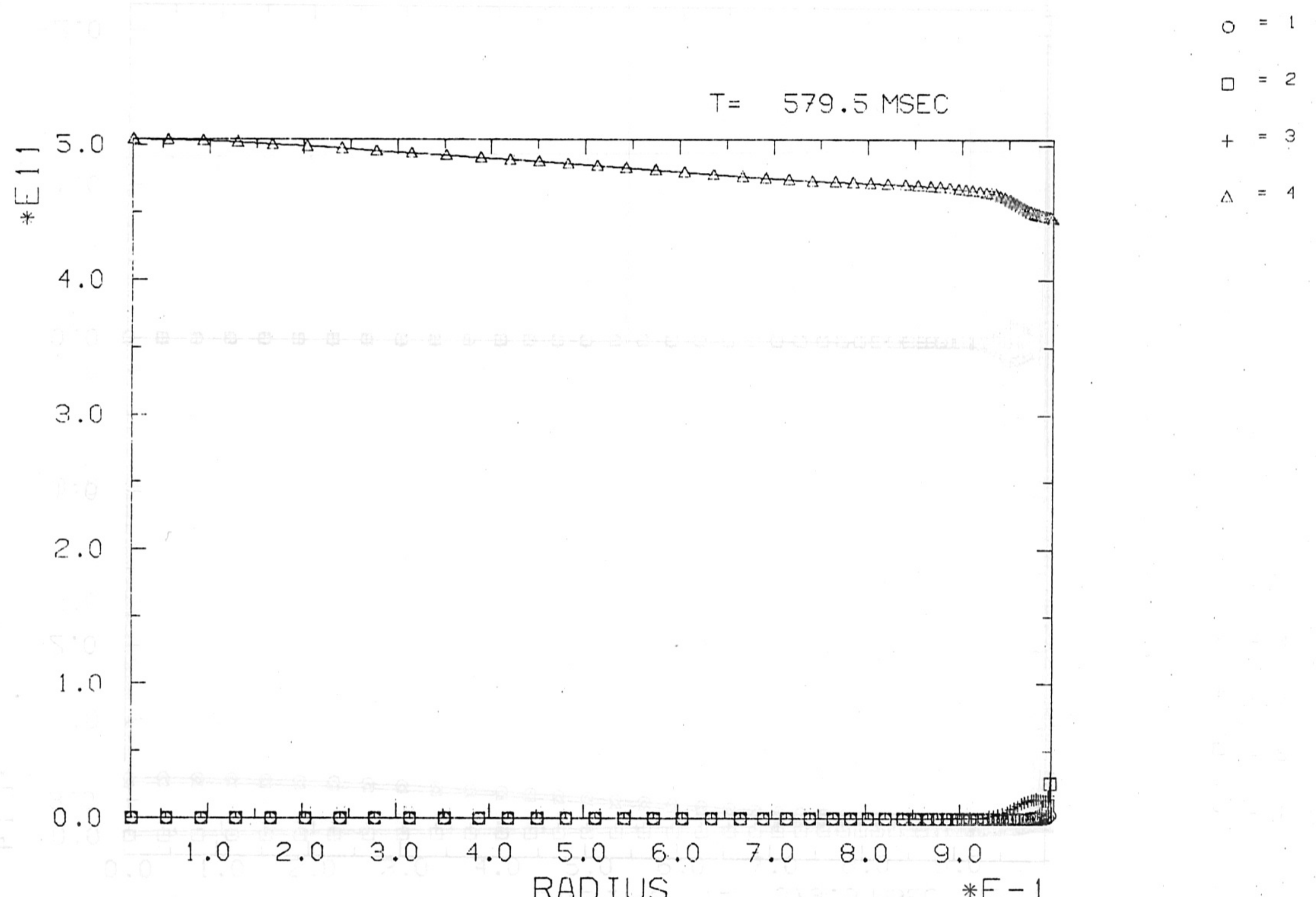

Fig.2(b) RADIAL PROFILES OF THE IMPURITY IONIZATION STATES

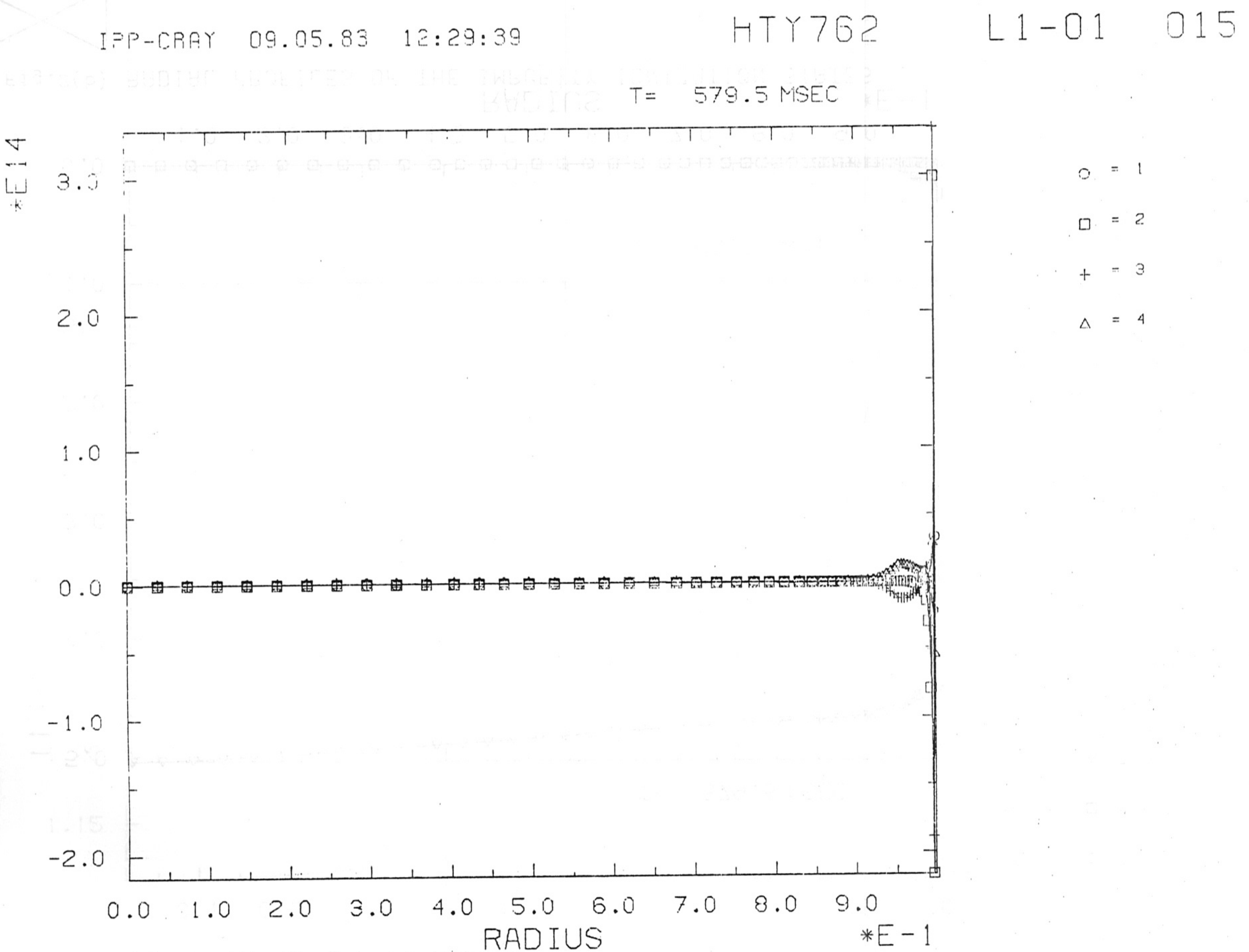

Fig.2(c) TOTAL PARTICLE FLUX DENSITY

IPP-CRAY 09.05.83 12:29:39 HTY762 L1-01 017

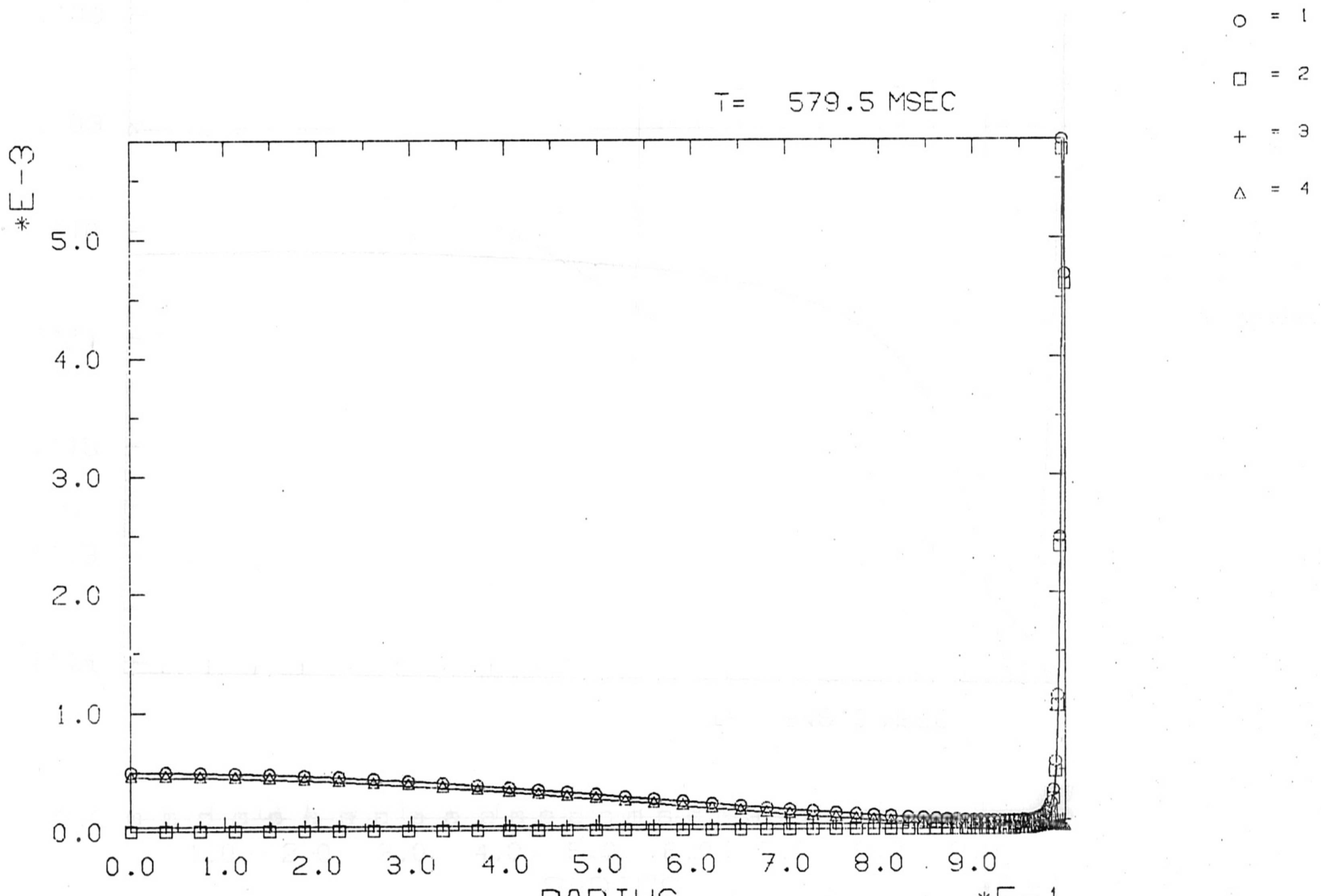

Fig.2(d) RADIATIVE ENERGY LØSS (PER UNIT VOLUME)-TOTAL.LINE.RECOM.BREMS

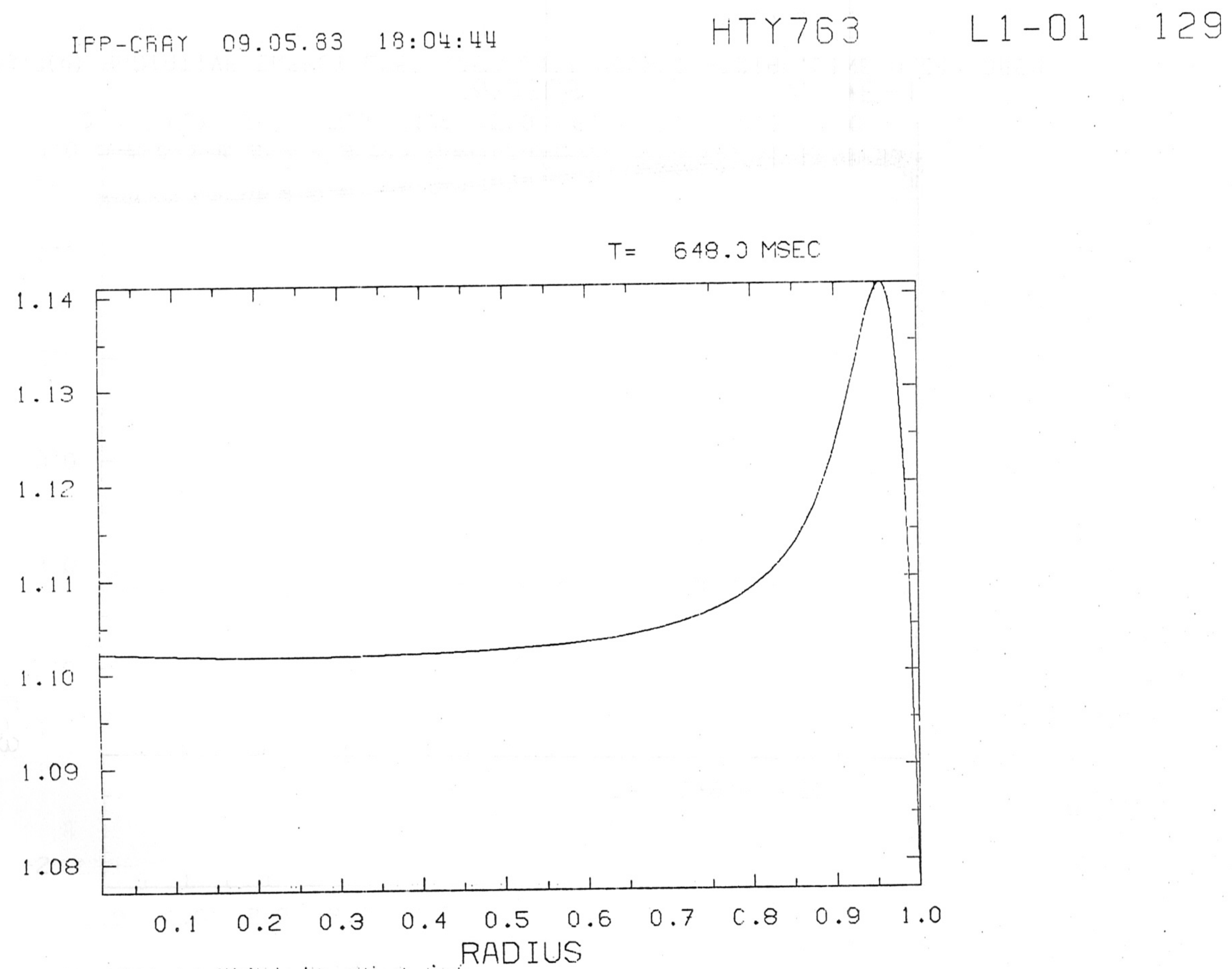

Fig.3(a) RADIAL PROFILES OF Z-EFF

IFP-CRAY 09.05.83 18:04:44 HTY763 L1-01 130

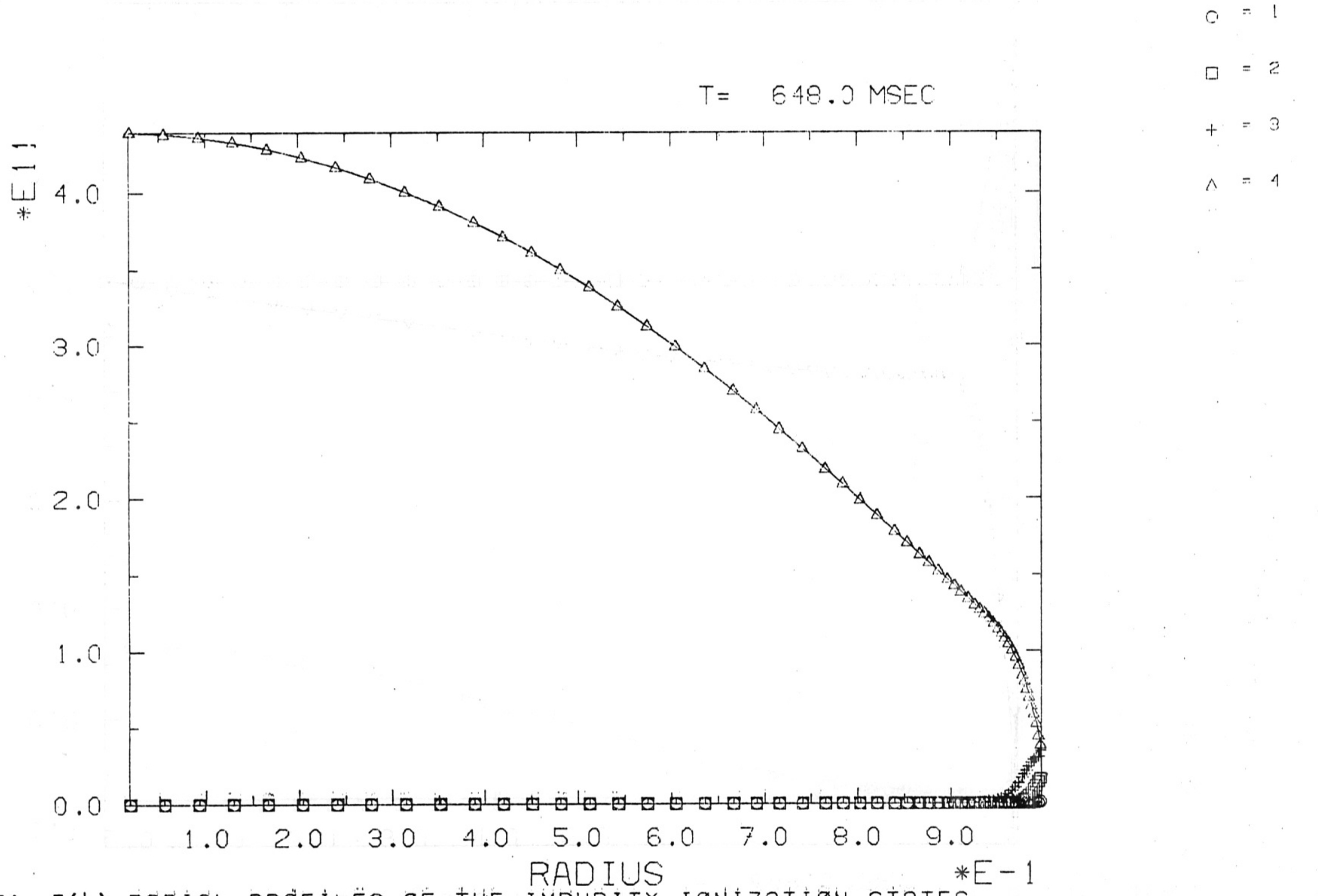

Fig.3(b) RADIAL PROFILES OF THE IMPURITY IONIZATION STATES

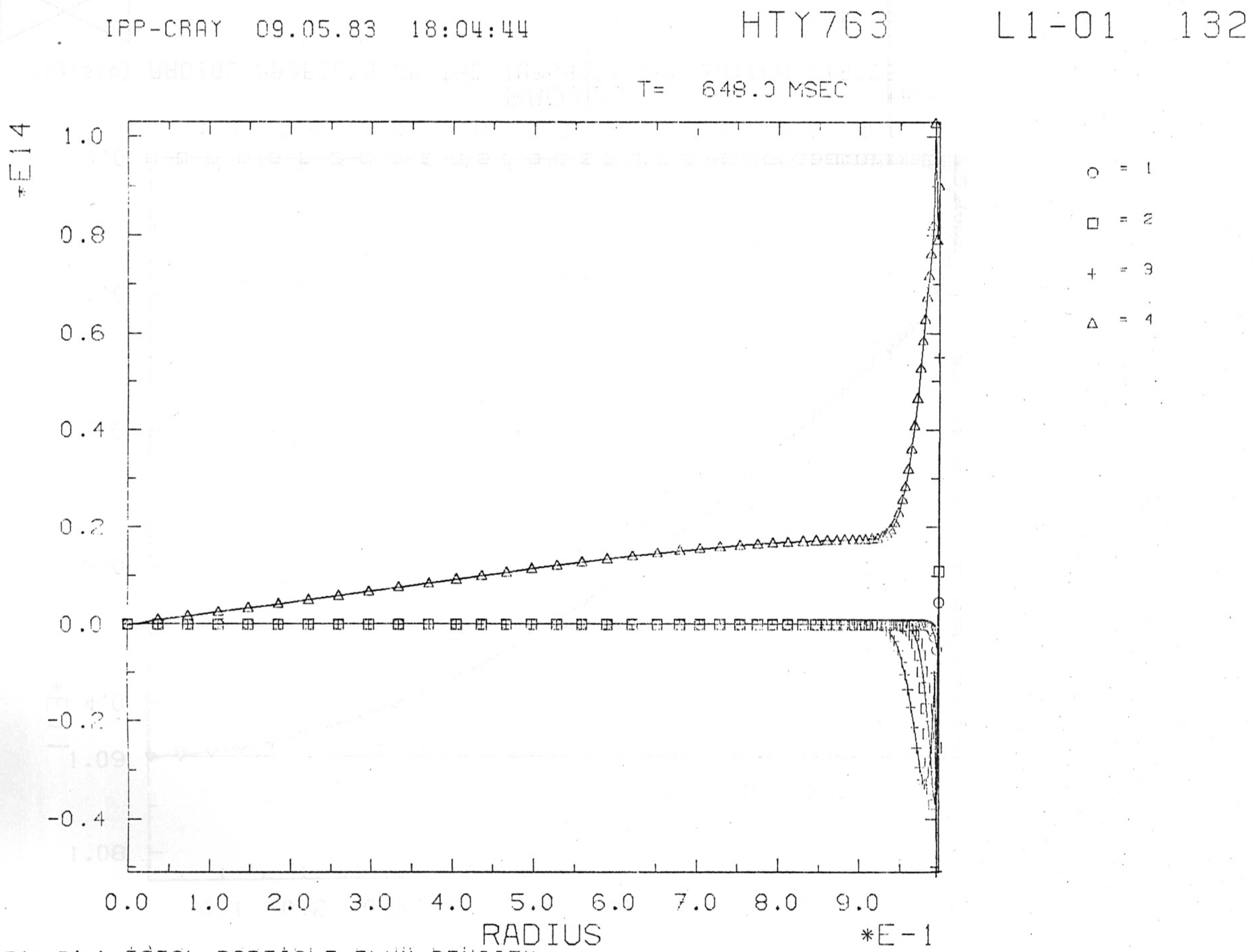

Fig.3(c) TOTAL PARTICLE FLUX DENSITY

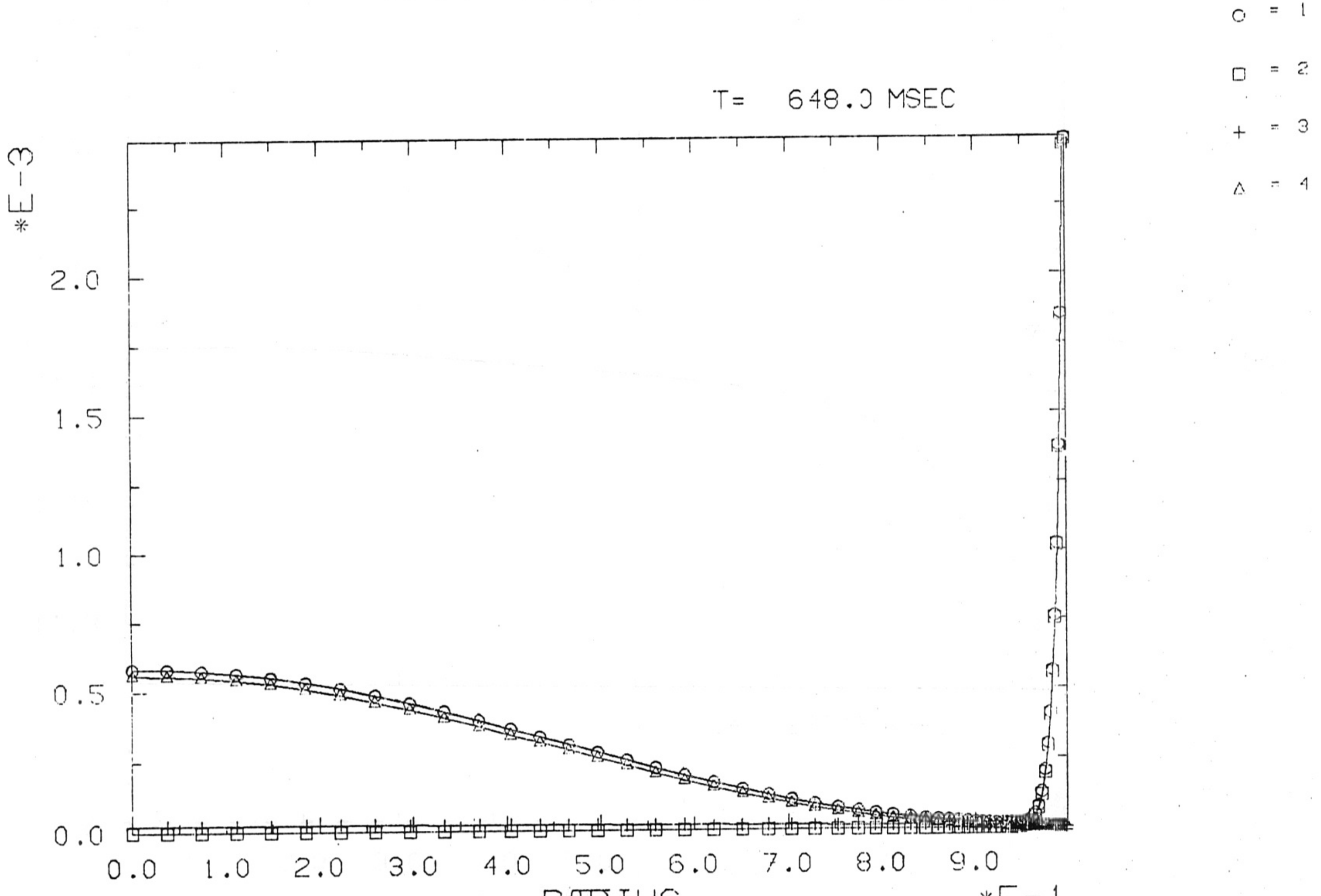

Fig.3(d) RADIATIVE ENERGY LOSS (PER UNIT VOLUME)-TOTAL.LINE.RECOM.BREMS

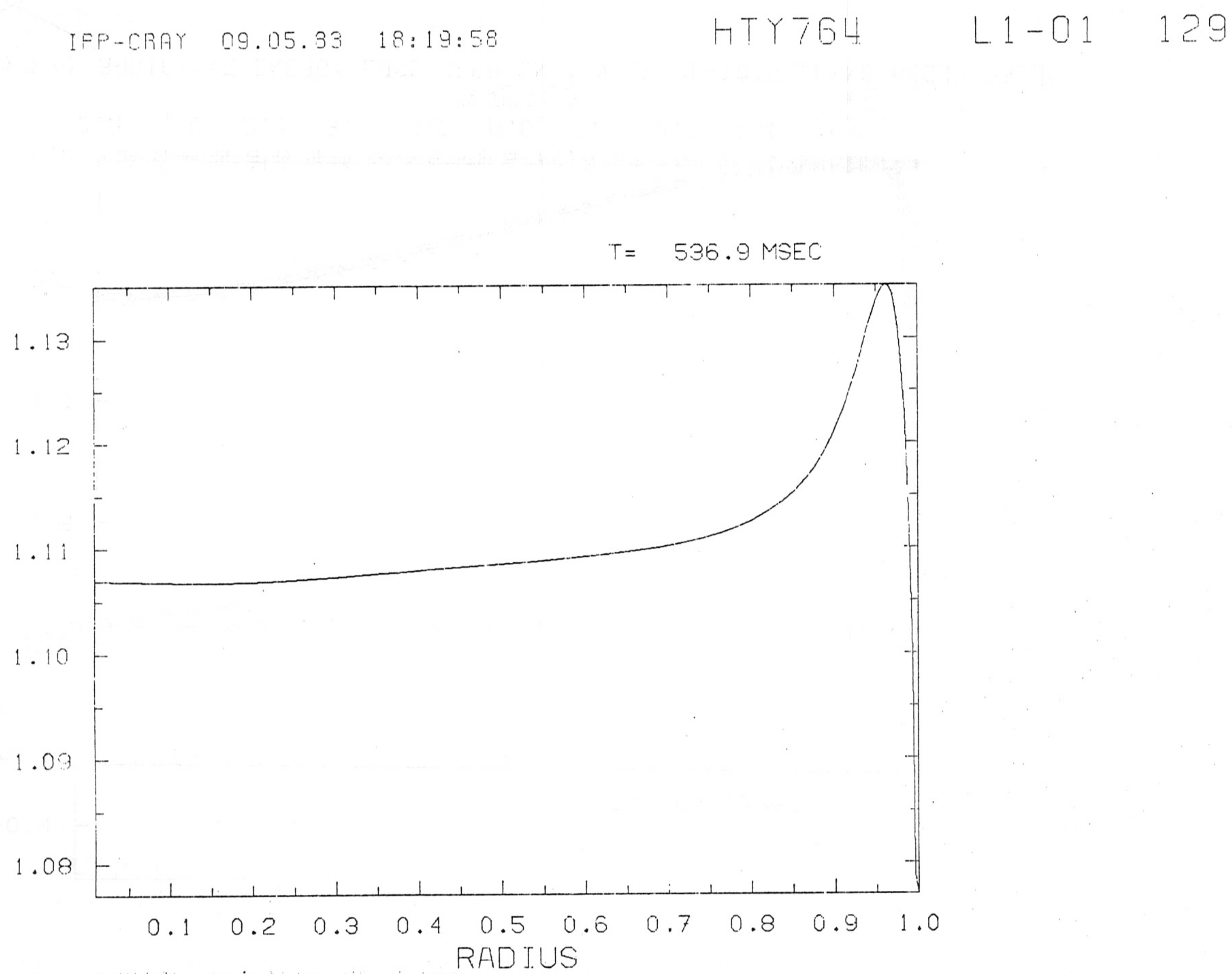

Fig.4(a) RADIAL PRØFILES ØF Z-EFF

IPP-CRAY 09.05.83 18:19:58 HTY764 L1-01 130

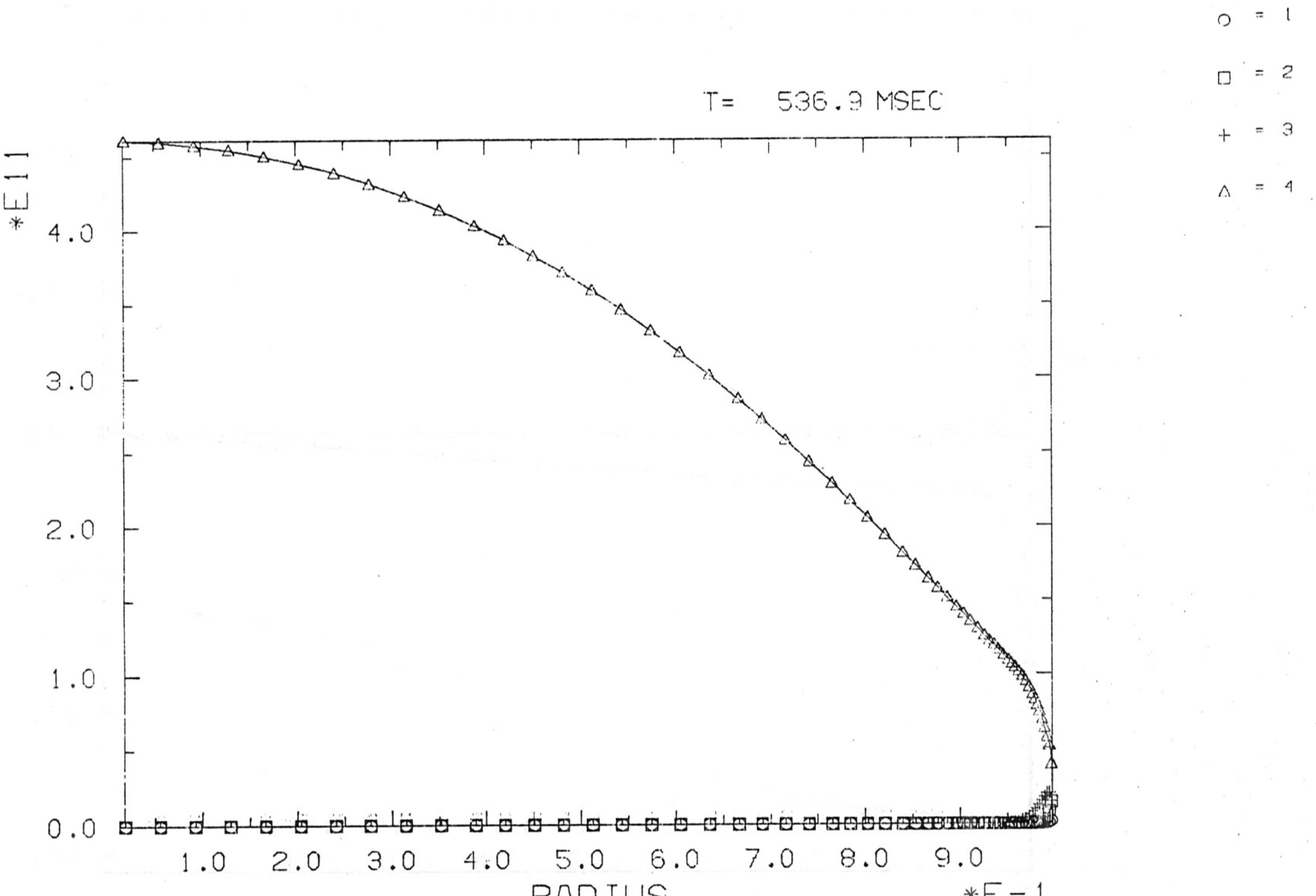

Fig.4(b) RADIAL PROFILES OF THE IMPURITY IONIZATION STATES

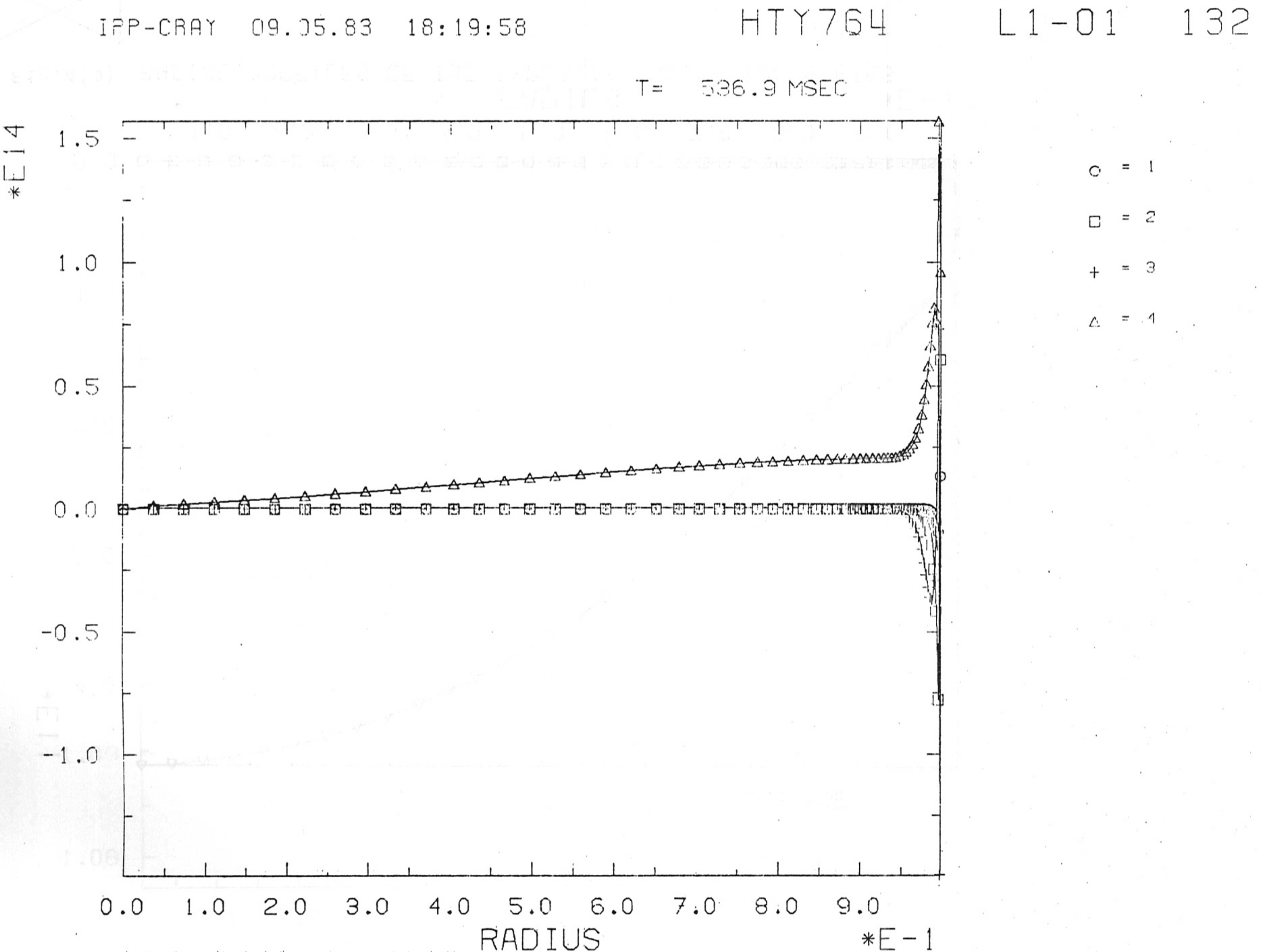

Fig.4(c) TOTAL PARTICLE FLUX DENSITY

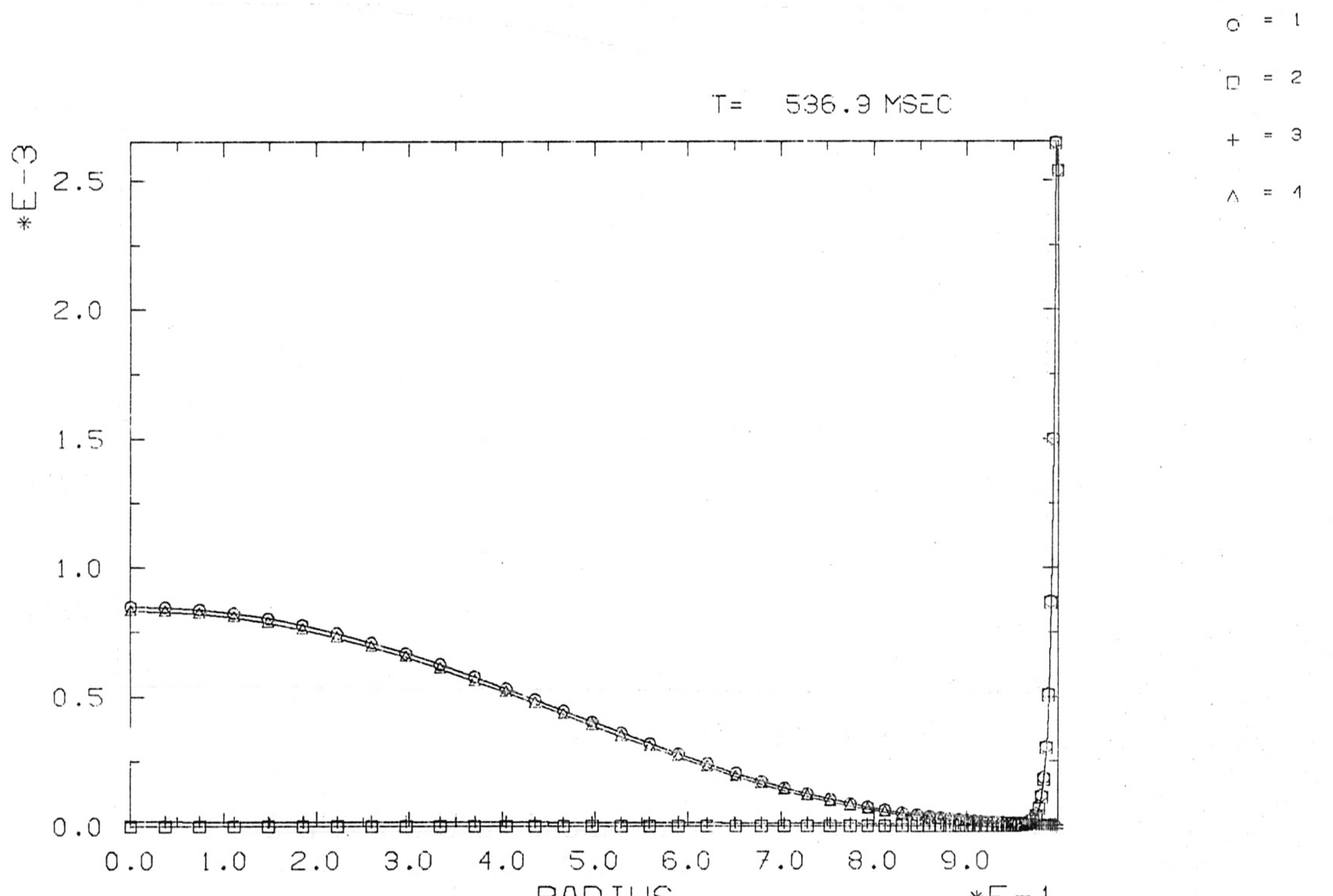

Fig.4(d) RADIATIVE ENERGY LOSS (PER UNIT VOLUME)-TOTAL.LINE.RECOM.BREMS

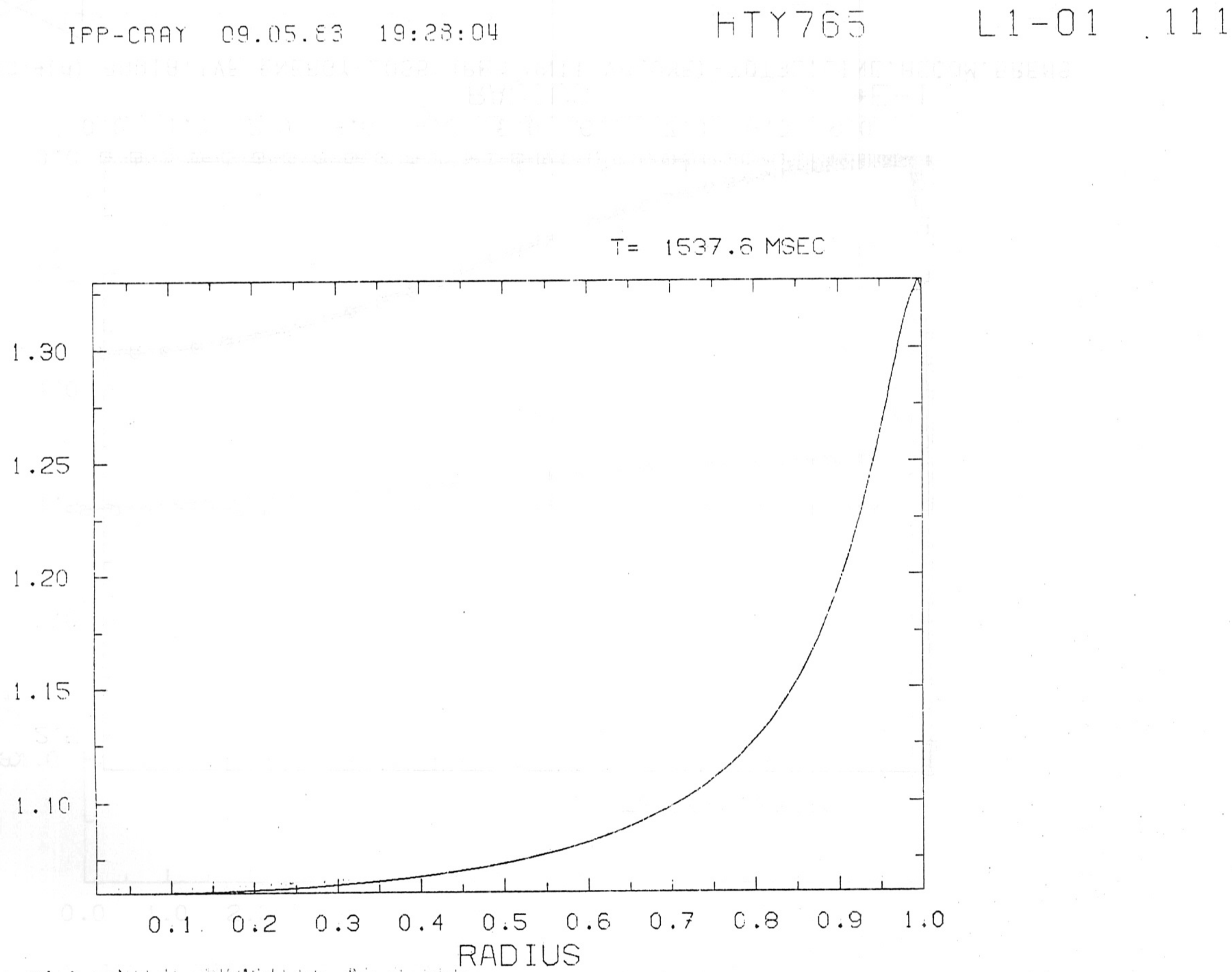

Fig.5(a) RADIAL PROFILES OF Z-EFF

IFP-CRAY 09.05.83 19:28:04 HTY765 L1-01 112

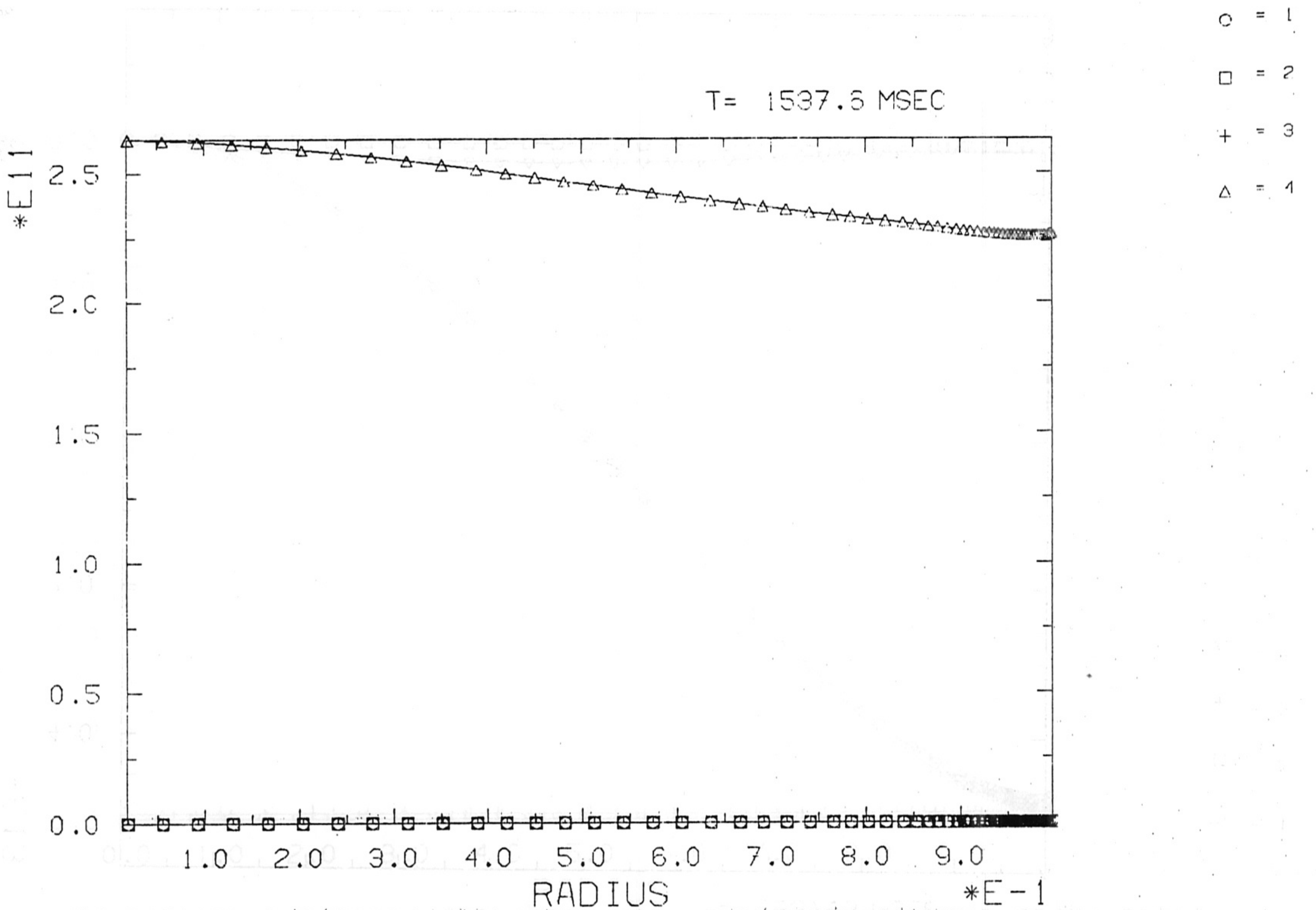

Fig.5(b) RADIAL PROFILES OF THE IMPURITY IONIZATION STATES

IPP-CRAY 09.05.83 19:28:04 HTY765 L1-01 114

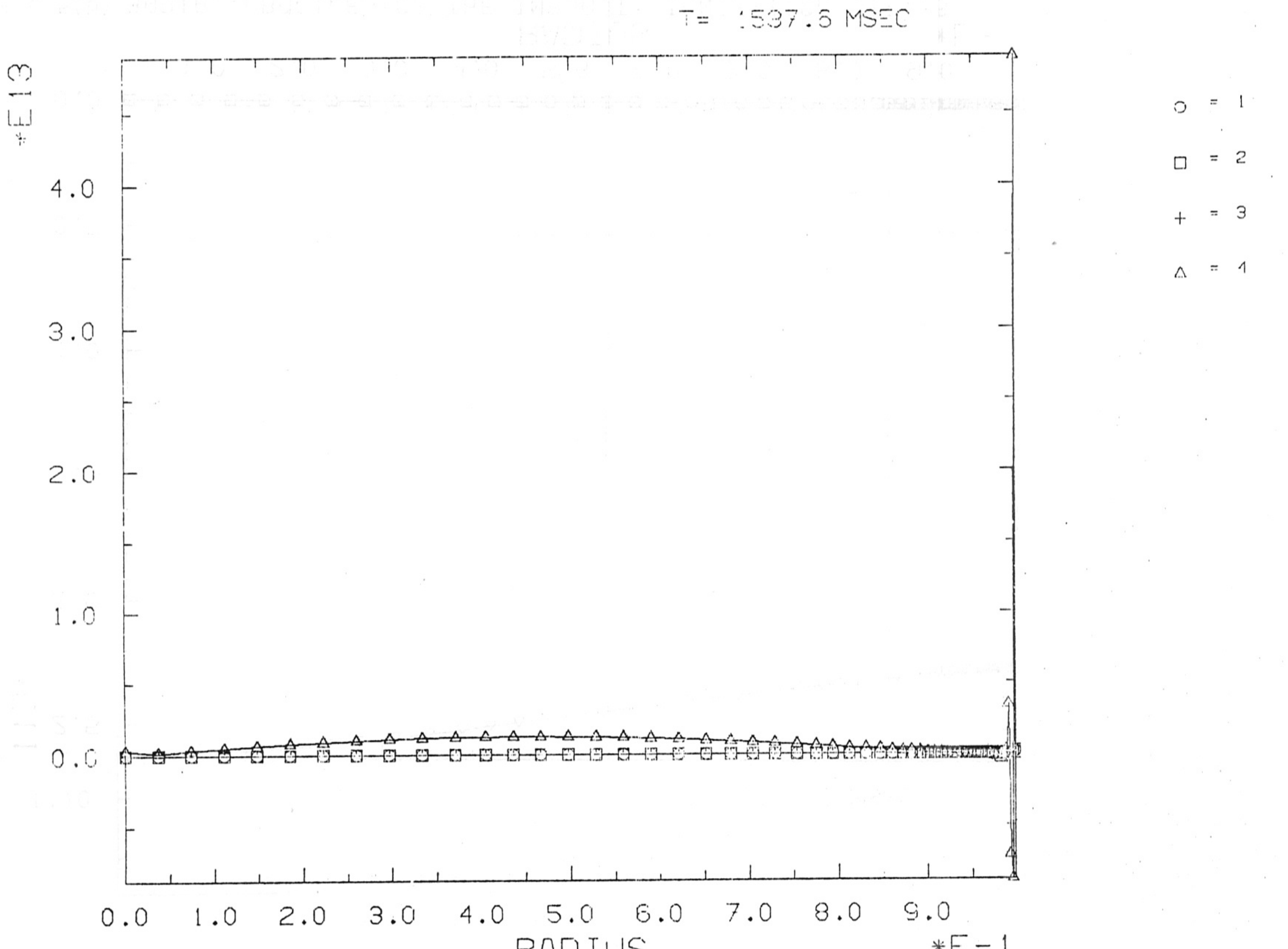

Fig.5(c) TOTAL PARTICLE FLUX DENSITY

IPP-CRAY 09.05.83 19:28:04 HTY765 L1-01 116

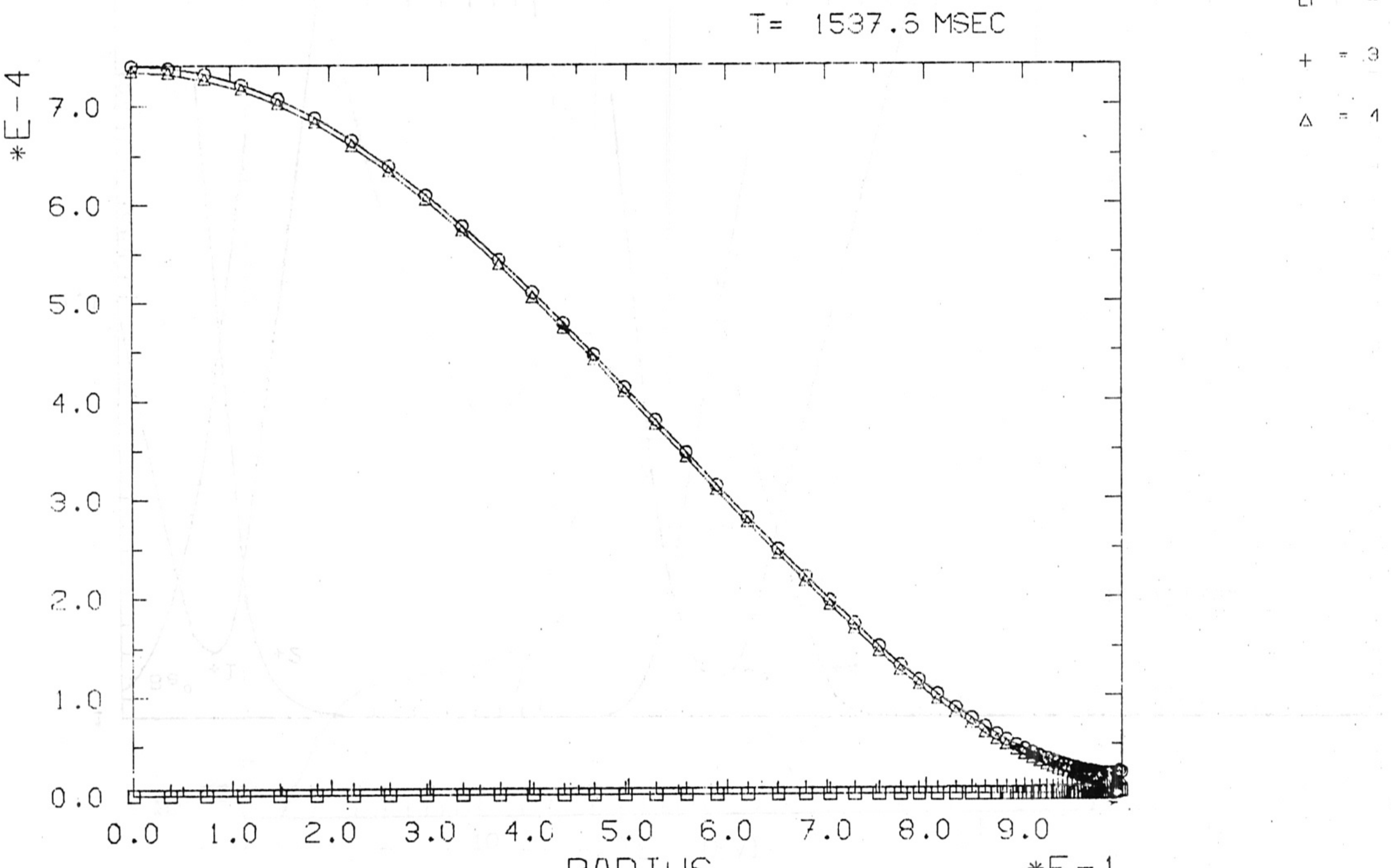

Fig.5(d) RADIATIVE ENERGY LOSS (PER UNIT VOLUME)-TOTAL.LINE.RECOM.BREMS

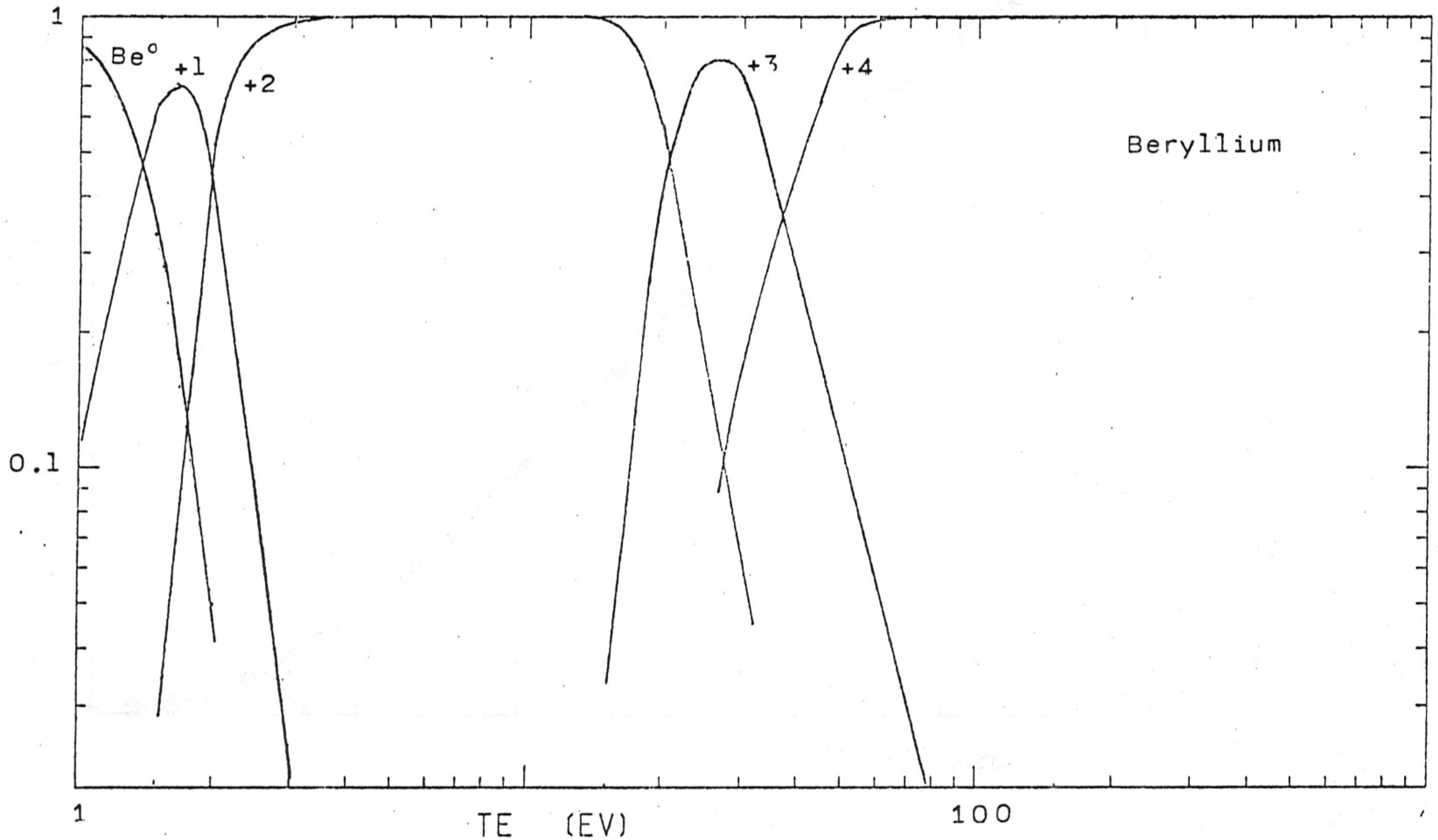

Fig.6 Fractional abundances of beryllium in corona equilibrium as a function of electron temperature.

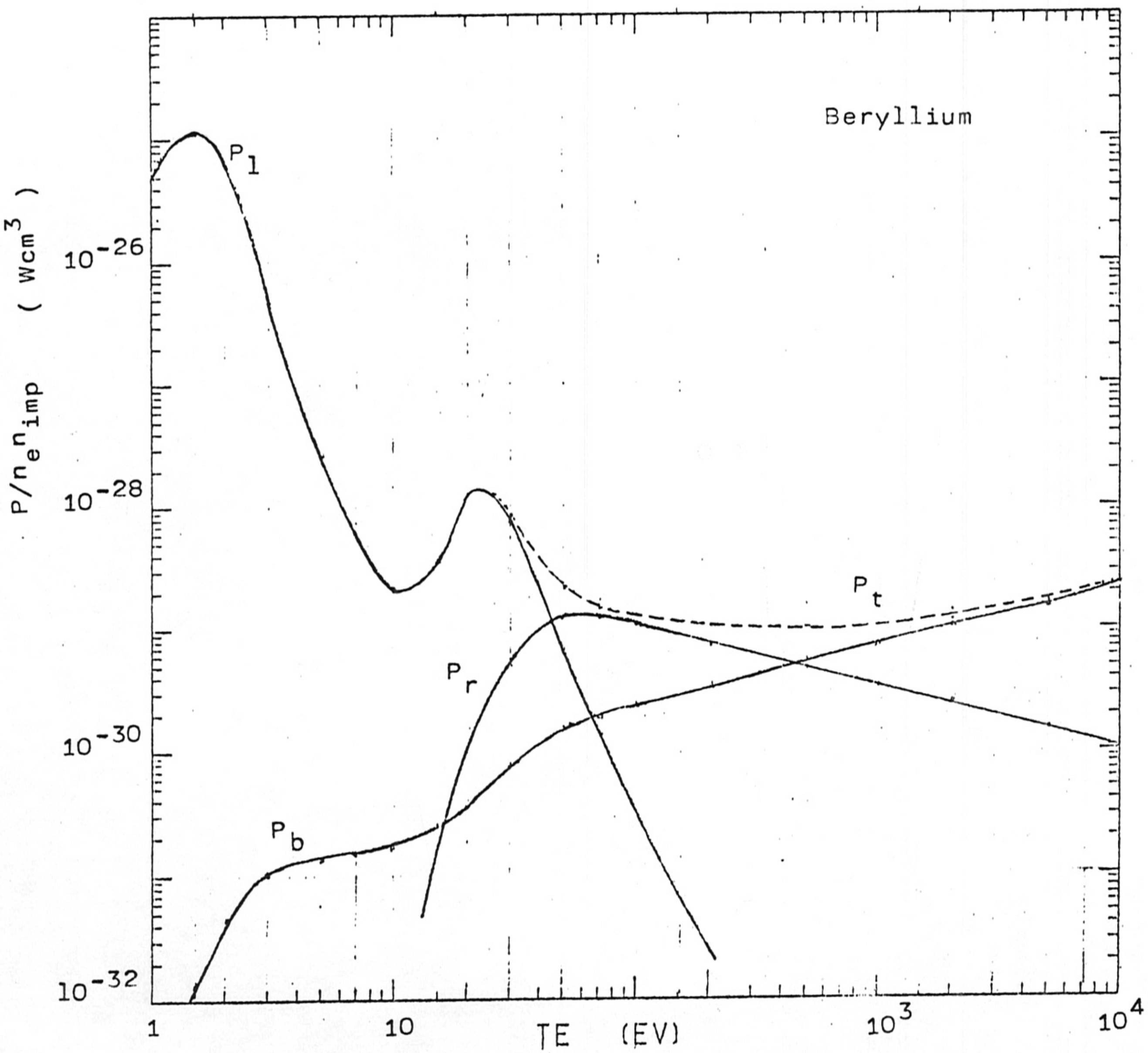

Fig.7 Radiation losses of beryllium at corona equilibrium as a function of electron temperature.